Published in final edited form as:
Cancer Res. 2013 January 15; 73(2): 571–582. doi:10.1158/0008-5472.CAN-12-0263.

CXCR2 expression in tumor cells is a poor prognostic factor and promotes invasion and metastasis in lung adenocarcinoma

Pierre Saintigny[1,+], **Erminia Massarelli**[1,+], **Steven Lin**[2,1], **Yulong Chen**[1], **Sangeeta Goswami**[1], **Baruch Erez**[2], **Michael S. O'Reilly**[2], **Diane Liu**[3], **J. Jack Lee**[3], **Li Zhang**[4], **Yuan Ping**[5], **Carmen Behrens**[5], **Luisa M. Solis Soto**[5], **John V. Heymach**[1], **Edward S. Kim**[1], **Roy S. Herbst**[7], **Scott M. Lippman**[1], **Ignacio I. Wistuba**[5], **Waun Ki Hong**[6], **Jonathan M. Kurie**[1], and **Ja Seok Koo**[7,*]

[1]Department of Thoracic/Head & Neck Medical Oncology, The University of Texas MD Anderson Cancer Center, Houston, Texas

[2]Department of Radiation Oncology, The University of Texas MD Anderson Cancer Center, Houston, Texas

[3]Department of Biostatistics and Applied Mathematics, The University of Texas MD Anderson Cancer Center, Houston, Texas

[4]Department of Bioinformatics and Computational Biology, The University of Texas MD Anderson Cancer Center, Houston, Texas

[5]Department of Pathology, The University of Texas MD Anderson Cancer Center, Houston, Texas

[6]Division of Cancer Medicine, The University of Texas MD Anderson Cancer Center, Houston, Texas

[7]Section of Medical Oncology, Yale Cancer Center, Department of Internal Medicine, Yale School of Medicine, 333 Cedar Street, New Haven, Connecticut.

Abstract

CXCR2 in non-small cell lung cancer (NSCLC) has been studied mainly in stromal cells and is known to increase tumor inflammation and angiogenesis. Here, we examined the prognostic importance of CXCR2 in NSCLC and the role of CXCR2 and its ligands in lung cancer cells. The effect of CXCR2 expression on tumor cells was studied using stable knockdown clones derived from a murine *KRAS/p53*-mutant lung adenocarcinoma cell line with high metastatic potential and an orthotopic syngeneic mouse model and *in vitro* using a CXCR2 small molecule antagonist (SB225002). CXCR2 protein expression was analyzed in tumor cells from 262 NSCLC. Gene expression profiles for *CXCR2* and its ligands (*CXCR2* axis) were analyzed in 52 human NSCLC cell lines and 442 human lung adenocarcinomas. Methylation of *CXCR2* axis promoters was determined in 70 human NSCLC cell lines. Invasion and metastasis were decreased in *CXCR2* knockdown clones *in vitro* and *in vivo*. SB225002 decreased invasion *in vitro*. In lung adenocarcinomas, CXCR2 expression in tumor cells was associated with smoking and poor prognosis. *CXCR2* axis gene expression profiles in human NSCLC cell lines and lung adenocarcinomas defined a cluster driven by *CXCL5* and associated with smoking, poor prognosis

[*]**Corresponding author:** Ja Seok Koo, Ph.D., Section of Medical Oncology, Yale Cancer Center, Department of Internal Medicine, Yale School of Medicine, 333 Cedar Street, New Haven, Connecticut; Phone: 203-737-6221; Fax: 203-737-5698; jpeter.koo@yale.edu.
[+]P.S. and E.M. contributed equally to this work.

Authors have no conflict of interest to disclose

and RAS pathway activation. Expression of *CXCL5* was regulated by promoter methylation. The *CXCR2* axis may be an important target in smoking-related lung adenocarcinoma.

Keywords

lung cancer; prognosis; metastasis; CXCR2; chemokine

Introduction

Adenocarcinoma represents the most common histologic subtype of lung cancer (1). The identification of *EGFR* mutations and *ALK* rearrangements has modified our approach to treating non-small cell lung cancer (NSCLC) (2). However, these single oncogenic driver mutations are mostly seen in lung adenocarcinoma from never smokers (3), and little progress has been made in the treatment of smoking-related lung adenocarcinoma. *KRAS* and *BRAF* driving mutations are more frequently seen in smokers, but the proportion of smoking-related lung adenocarcinoma with unknown driving mutations is high (4) and the identification of potential targets in this setting urgently needed.

Chemokines are small chemotactic cytokines mediating communication between different cell types (5). CXCR2 (IL8R) is a member of the G-protein–coupled receptor superfamily, and the receptor of Glu-Leu-Arg (ELR+) CXC chemokines: CXCL1, CXCL2, CXCL3, CXCL5, and CXCL7 (PPBP) bind specifically to CXCR2; CXCL6 and CXCL8 (IL8) are shared ligands of CXCR1 and CXCR2. CXCR2 expression has been demonstrated in neutrophils, monocytes, eosinophils, mast cells, basophils, lymphocytes, epithelial cells, and endothelial cells (5, 6). CXCR2 inhibitors are currently under development in chronic obstructive pulmonary disease (COPD), with the rationale of inhibiting pulmonary damage by neutrophils, goblet cell hyperplasia, and angiogenesis caused by smoking (6, 7). We have previously reported that alveolar epithelial cells transformed by oncogenic *KRAS* express high levels of CXCR2 ligands, which recruit inflammatory and endothelial cells and promote progression of premalignant alveolar lesions to lung adenocarcinoma (8).

Neutrophils expressing CXCR2 infiltrate the tumor microenvironment. CXCR2 expression in endothelial cells is activated by ELR+ CXC chemokines that are potent proangiogenic factors and promote tumor growth (9-13). However, the role of CXCR2 in tumor cells is debated. *In vitro*, it has been shown to promote cell proliferation, migration, and invasion (14-17) and to assist cancer cells in evading stress-induced apoptosis (18). CXCR2 inhibitors have been reported to decrease tumor growth. However, whether this effect is mediated mainly by inhibition of angiogenesis and/or by a direct effect on tumor cells remains unclear (10, 16, 19, 20). On the other hand, it has been reported recently that depletion of CXCR2 both delays replicative senescence and impairs the senescence response to oncogenic signals, suggesting that it acts as a tumor suppressor (21).

These results may reflect multiple pro- and anti-tumorigenic actions depending on tumor type and stage. To clarify the role of CXCR2 in NSCLC and help characterize its role as a potential target in NSCLC, we hypothesized that CXCR2 expression by tumor cells promotes tumor invasion and metastasis in NSCLC. To test this hypothesis, we studied the functional role of CXCR2 *in vitro* in a model of *KRAS*/*p53*–mutant lung adenocarcinoma, *in vivo* in an orthotopic syngeneic mouse model (22-24), and analyzed the association of CXCR2 expression in human NSCLC cells with clinicopathological characteristics. Furthermore, we performed a systematic analysis of gene expression profiles of *CXCR2* and its ligands (subsequently called the *CXCR2* axis) in human NSCLC cell lines and lung adenocarcinoma.

Material and Methods

Human lung tissues and tissue microarray

A detailed description of the tissue microarray construction is provided elsewhere (25). In summary, after histological examination of NSCLC specimens, the NSCLC TMAs were constructed by obtaining three 1-mm in diameter cores from each tumor at three different sites (periphery, intermediate and central tumor sites).

Immunohistochemical analysis

Mouse monoclonal anti-human CXCR2 antibody (R&D Systems, Minneapolis, MN) was used at a dilution of 1:200, according to the manufacturer's instruction. CXCR2 staining was examined using light microscopy by a lung cancer pathologist (Y.P.). An independent observer (I.I.W) reviewed one third of the cores chosen randomly. In case of discordance (~10%), both pathologists reviewed the slides jointly in a multiheaded microscope and reached consensus. Both pathologists were blinded with respect to the patients' outcome. Only cytoplasmic CXCR2 expression was quantified using a four-value intensity score (0, 1+, 2+, and 3+) and extent of reactivity (0-100%). Final score was then obtained by multiplying the intensity and reactivity extension values (range, 0-300).

Animal husbandry

All animal experiments were reviewed and approved by the Institutional Animal Care and Use Committee at MD Anderson Cancer Center. For syngeneic tumor experiments, 10- to 16-week-old 129/Sv mice were injected with the indicated numbers of tumor cells into the left lung and euthanized at the first signs of morbidity.

Establishment of murine lung adenocarcinoma cell lines

The methods used to establish lung adenocarcinoma cell lines in culture from murine tumors have been described previously (22). Cell lines were named according to the mouse number and site of derivation (e.g., 344SQ for mouse 344, subcutaneous metastasis). These cells have alveolar type II cell properties and variable propensities to undergo the epithelial-to-mesenchymal transition and metastasize following injection into syngeneic mice (22, 24).

RNA extraction and quantitative reverse-transcription PCR

RNAs were extracted using TRIzol (Invitrogen, Carlsbad, CA). mRNA was reverse-transcribed using the SuperScript First-Strand Synthesis System (Invitrogen). For quantitative PCR reactions, 1:10 dilutions of cDNA products were amplified by using SYBR Green PCR Master Mix (Applied Biosystems, Carlsbad, CA) and analyzed by using ABI Prism 7500 Fast System (Applied Biosystems). mRNA expression values were normalized on the basis of L32 mRNA.

Generation of shRNA transfectants

The shRNA retroviral *CXCR2* constructs were purchased (OriGene, Rockville, MD). The sequences of the CXCR2 and scrambled shRNA were as follow: CAAGGTGGATAAGTTCAACATTGAAGATT (CXCR2 clone 1), GTCTGCTATGAGGATGTAGGTAACAATAC (CXCR2 clone 3), and GCACTACCAGAGCTAACTCAGATCGTACT (scrambled shRNA). Purified plasmids (1 μg of each) were transfected into 344SQ cells by using LipofectAmine and PLUS (Invitrogen). After 48 hours, transfectants were replated in RPMI 1640 medium containing 10% FBS and 15 μg/ml puromycin for selection and passed serially for 4 weeks to generate stable transfectants.

Cell invasion assay

As described previously (22), cells (cancer-associated fibroblasts) were seeded first in the lower chambers (10^5 cells), and tumor cells (344SQ) were then seeded in the upper chambers (5×10^4) of 24-well Transwell invasion plates (BD Biosciences, Bedford, MA) in serum-free medium containing mitomycin C to block proliferation. Cells in the upper chambers were allowed to invade for 14 to 16 hour,. Cells on the inserts were fixed with 90% ethanol, stained with 0.1% crystal violet blue, and washed with ddH_2O. Noninvaded cells on the upper side of the inserts were wiped off with a cotton swab. Invaded cells were counted in five microscopic fields at 4× magnification, and the counts were averaged.

A small molecule antagonist of CXCR2 (SB225002) (Calbiochem) was used to inhibit CXCR2 invasive properties of 344P cells in Boyden chamber assays and included 344SQ cells as positive controls (26, 27).

Gene expression analysis

Publicly available gene expression profiles and clinical annotations of 442 lung adenocarcinomas were downloaded from the NCI Director's Challenge Consortium for the Molecular Classification of adenocarcinoma (DCC) (28). CEL files of 52 NSCLC cell lines (GSE4824) (29, 30), 130 lung squamous cell carcinomas with clinical annotations (GSE4573) (31), and 7 NSCLC cell lines and 3 human bronchial epithelial cell lines (HBEC) before and after treatment with 5-aza-2′-deoxycytidine (decitabine) (GSE5816) (32) were downloaded from Gene Expression Omnibus (GEO).

The gene expression analysis was generated by using Array Studio software (Omicsoft Corporation, Research Triangle Park, NC). Raw microarray data were processed using quantile normalization and robust multi-array average algorithm. Probesets corresponding to *CXCR2* axis were identified using the NetAffx Analysis Center from Affymetrix website. They were used to compute an unsupervised hierarchical clustering of the cell lines and of the lung adenocarcinomas using the Pearson's correlation coefficient and Ward's linkage method.

To summarize the effect of *CXCR2* axis, a principal component analysis was computed with the first two components. In the DCC, the first principal component (PC1) was used for correlative studies with tumor differentiation, smoking status, and overall survival. In the cell lines, PC1 was correlated with the whole genome. Gene Set Enrichment Analysis (GSEA) using the "pre-ranked" tool was done using either the genes ranked according to their correlation with PC1, or to fold-change between groups defined by the unsupervised hierarchical clustering. Probesets with an absolute Pearson correlation or a fold-change ≥0.5 were included in network analyses performed using Ingenuity Pathway Analysis (IPA) (Ingenuity® Systems, Redwood City, CA). Details of the GSEA and IPA are provided in Supplementary Material and Methods.

CXCL5 *promoter methylation study*

CXCL1, CXCL2, CXCL3, CXCL5 and *CXCL6* promoter methylation status was obtained from high-throughput promoter methylation profiles of 42 NSCLC cell lines overlapping with the panel of 52 NSCLC cell lines analyzed for gene expression. *CXCL7* and *CXCL8* results did not pass the quality control and were not included in the analysis. DNA methylation status of a set of 27,579 CpG sites around promoters of 14,475 consensus coding sequences was interrogated using the Illumina HumanMethylation27 Beadchip (Illumina, Inc., San Diego, CA). Genomic DNA (1 μg) was bisulfite-converted using the EZ DNA Methylation kit (Zymo Research Corp, Orange CA). Whole-genome amplification, fragmentation, hybridization, washing, counterstaining, and scanning were performed

according to the manufacturer's instructions. The scanner data and image output files were managed with the Illumina BeadStudio software Methylation module v.3.2. The normalized data, presented as beta values, represent the degree of methylation at each CpG site, 0 being unmethylated and 1 being methylated.

Statistical analysis

Wilcoxon rank sum test or Kruskal-Wallis test was used to test the differences of CXCR2 expression between/among categorical variable levels. Martingale residuals were performed from a Cox model that included only baseline hazard function but no covariate. By applying a nonparametric smoother, the plots allow one to examine visually the nature of the relationship between the residuals and CXCR2 H-scores and to define a reasonable cutoff point to dichotomize the population. The Kaplan-Meier method was used to construct overall and recurrence-free survival curves, and the log-rank test was used to test the difference by covariate levels. Univariate and multivariate Cox models were fitted to estimate the effect of prognostic factors, including patient age, sex, tumor histology, stage, and marker on time to event endpoint. For cell line experiments, comparisons between two groups were performed using the Wilcoxon rank sum test unless otherwise indicated. One-way ANOVA was performed to compare multiple experimental groups. All statistical tests were two-sided, and *P*-values of 0.05 or less were considered to be statistically significant.

Results

Creation of an orthotopic syngeneic lung adenocarcinoma metastasis model

We recently described the creation of a panel of cell lines from $Kras^{LA1/+}p53^{R172H\Delta G/+}$ mice, which develop aggressive and metastatic lung adenocarcinoma (24). One of these cell lines, 344SQ, is highly metastatic when injected subcutaneously into syngeneic mice (22). In order to refine our lung adenocarcinoma metastasis model, we used 344SQ to create a novel orthotopic syngeneic model. As previously described (33), 2×10^4 344SQ cells were injected into the left lung of syngeneic mice. The mice were euthanized 21 days after injection and, at necropsy, had developed metastases to hilar and mediastinal lymph nodes (Fig. 1), chest wall, and controlateral lung as well as extrathoracic distant metastases in the paraaortic lymph nodes, liver, adrenal glands, kidneys, spleen and diaphragm.

CXCR2 knockdown decreased tumor cell invasion in vitro

To investigate the role of CXCR2 expression by tumor cells, we created *CXCR2* shRNA clones from parental 344SQ lung adenocarcinoma cell lines isolated from $Kras^{LA1/+}p53^{R172H\Delta G/+}$ mice. *CXCR2* shRNA clones exhibited significantly lower expression of *CXCR2* mRNA than scrambled controls (Fig. 2A). To test the invasion potential of the shRNA clones, we used co-cultures with cancer-associated fibroblasts, which produce high levels of CXCR2 ligands, as previously described (34). To block tumor cell proliferation, we added mitomycin C to the serum-free medium in which the tumor cells were cultured (344SQ). *CXCR2* shRNA clones showed a significantly lower invasion potential than scrambled controls (Fig. 2B).

CXCR2 pharmacological inhibition decreased tumor cell invasion in vitro

To confirm our findings in the 344SQ cells, we carried out experiments by using 344P, a second highly invasive and metastatic lung adenocarcinoma cell line derived from $Kras^{LA1/+}p53^{R172H\Delta G/+}$mice. To inhibit CXCR2 using a different approach, we used a small molecule antagonist of CXCR2, SB225002, that has demonstrated selectivity and potency *in vitro* and *in vivo (26, 27).* We examined the effect of SB225002 on 344P cell invasive properties in Boyden chamber assay and included 344SQ cells as a positive control.

Treatment with SB225002 inhibited tumor cell invasive properties with as IC_{50} of 3-4 μM for both 344P cells and 344SQ cells (Fig. 2C-D).

CXCR2 knockdown in tumor cells decreased 344SQ metastatic potential

We used the orthotopic murine model already described to test whether the metastatic potential of 344SQ would be affected by *CXCR2* knockdown. Two shRNA clones (clone-1 and clone-3) and scrambled controls were compared by injecting 2×10^4 cells into the left lung of mice (N=10 in each group, for a total of 30 mice). Mice were euthanized at 21 days after injection because two of the 10 mice in the scrambled control group demonstrated poor physical conditions due to tumor burden. At necropsy, mice bearing *CXCR2*-shRNA lung adenocarcinoma had significantly fewer lung tumor nodules in the lung of primary injection (Fig. 2E) and fewer distant metastases (Fig. 2F) than scrambled controls. Sites of distant metastases included liver, adrenal glands, ipsilateral and controlateral lung, diaphragm, spleen and paraortic lymph nodes.

CXCR2 protein expression in human NSCLC tumor cells is associated with adverse outcome and tobacco smoking

To investigate the role of CXCR2 in human tumor cells, we stained a tissue microarray that included 370 resected NSCLC. For the purpose of this study, we considered only 262 patients with stage I and II disease who did not receive preoperative chemotherapy. Clinical and pathological characteristics of the patient population are described in Table 1. Median age was 67.4 years (range: 32.2-90.0). Adenocarcinoma was the most frequent histological subtype (N=173, 66%). With a median follow-up of 5.3 years, 133 patients had developed recurrence (50.8%) and 101 had died (38.5%). CXCR2 was expressed mainly in the cytoplasm (mean 31.07±30.78, median 20, range 0-130). Distribution of cytoplasmic CXCR2 protein expression in the whole population is shown in Supplementary Fig. 1A. Figure 3 shows one adenocarcinoma and one squamous cell carcinoma expressing CXCR2 with an intensity of 1 in 100% of tumor cells, and an H-score of 100. CXCR2 expression was low in the nucleus (mean 16.15±24.88, median 3.33, range 0-120). Cytoplasmic and nuclear CXCR2 expression levels were not correlated (rho=−0.02, P=0.76). No association was observed between cytoplasmic CXCR2 and patient sex, race, tumor histology, stage or degree of inflammation. Cytoplasmic CXCR2 expression was higher in current smokers (32.57±28.28) and former smokers (31.19±33.15) than in never smokers (25.28±29.00), although it did not reach statistical significance. Similarly, poorly differentiated tumors had higher cytoplasmic CXCR2 levels (39.84±32.20) than moderately (29.99±30.18) or well-differentiated (16.46±23.98) tumors ($P<0.0001$). The Martingale residual plots showed that median CXCR2 H-score was a reasonable cutoff point (Supplementary Fig. 1B). When cytoplasmic CXCR2 level was dichotomized using the median expression of 20, 141 (53.8%) tumors expressed low CXCR2 levels (<=20) and 121 (46.2%) tumors expressed high CXCR2 levels (>20). *EGFR* and *KRAS* mutational status was available for 157 of the lung adenocarcinomas; Supplementary Fig. 2 shows that cytoplasmic CXCR2 protein expression was lower, although not reaching statistical significance, in *EGFR*-mutant lung adenocarcinomas (N=17, mean 24.71±29.49, median 13.33, range 0-90), which are known to be more frequent among never smokers, than in *KRAS*-mutant (N=41, mean 31.02±31.65, median 20, range 0-110) or wild-type *EGFR* and wild-type *KRAS* lung adenocarcinomas (N=99, mean 33.05±33.61, median 20, range 0-130), which are more frequent among smokers.

Using Kaplan-Meier curves, high CXCR2 expression was associated with poor overall survival and recurrence-free survival in patients with lung adenocarcinoma, although not reaching statistical significance (Fig. 3C-D). No such association was observed in patients with squamous cell carcinoma (Supplementary Fig. 3A-B). Univariate Cox proportional

hazards model assessed the effect of covariates on survival. High CXCR2 expression was associated with worse overall survival in both subtypes [hazard ratio (HR) =1.488 95% confidence interval (95%CI): 0.905-2.448; HR=1.520 95%CI: 0.798-2.894] (Supplementary Table 1A and 2A), although not reaching statistical significance. For recurrence-free survival, a similar trend was observed in adenocarcinoma (HR=1.284 95%CI: 0.830-1.985), but not in squamous cell carcinoma (HR=1.028 95%CI 0.593-1.782) (Supplementary Table 1B and Table 2B). Final multicovariate Cox models are presented in Table 2. Combining all patients together, after adjusting for patients' age, sex, and tumor stage, high cytoplasmic CXCR2 expression remained associated with poor overall survival (HR=1.559; 95%CI: 1.051-2.312, P=0.0273) (Table 2A).

Gene expression pattern of CXCR2 axis is associated with human smoking-related adenocarcinoma and adverse clinical features

High-throughput gene expression profiles offer the opportunity to study *CXCR2* as well the genes that encode for its known ligands. We took advantage of publicly available profiles of 52 NSCLC cell lines and 442 early stage resected lung adenocarcinoma. Gene expression patterns of *CXCR2* ligands in NSCLC cell lines and lung adenocarcinoma were comparable (Supplementary Fig. 4). Unsupervised hierarchical clustering using the *CXCR2* axis identified a cluster of cell lines with high expression of CXCR2 ligand genes, which we called the *CXCR2/CXCR2* ligands cluster, that included nine (17%) of the cell lines analyzed (Fig. 4A). This group was enriched in *KRAS* mutations (Fisher's exact test, *P*=0.0548). HCC827, an *EGFR*-mutant cell line with an exon 19 deletion, was also part of this group. In lung adenocarcinomas, a similar cluster of 115 (26%) tumors was identified (Fig. 4B). *EGFR* mutation status was available for 170 adenocarcinomas. None of the 30 tumors included in the *CXCR2/CXCR2* ligands cluster harbored *EGFR* mutations, whereas 24 of the remaining 140 adenocarcinomas did harbor an *EGFR* mutation (Fisher's exact test, *P*=0.0295). A similar *CXCR2/CXCR2* ligands cluster was observed in each of the four individual cohorts forming the DCC (data not shown). A trend toward a worse prognosis in the high *CXCR2/CXCR2* ligands cluster was observed (Supplementary Fig. 5A). Using a similar approach in 130 patients resected for squamous cell carcinoma and included in the GEO series GSE4573 (31), we did not see any association between high CXCR2/CXCR2 ligands cluster and poor outcome (Supplementary Fig. 5B,C).

In both cell lines and lung adenocarcinoma, we compared the genes differentially expressed between the *CXCXR2/CXCR2* ligands cluster and the remaining samples across the whole genome. Probesets with an absolute fold-change ≥0.5 and a *P*-value ≤0.05 in both cell lines and lung adenocarcinoma are provided in Supplementary Results. In both cases, *CXCL5* gene was the most frequently upregulated in the *CXCR2/CXCR2* ligands cluster. Members of the aldo/keto reductase superfamily (*AKR1B10, AKR1C2, AKR1C3*), associated with tobacco exposure, were also upregulated.

In cell lines, *TGFB1*, vimentin (*VIM*), and osteopontin (*SPP1*) were upregulated in the *CXCR2/CXCR2* ligands cluster, while desmoplakin (*DSP*) and hepatocyte growth factor activator inhibitor 1 (*SPINT1*) were downregulated. These changes may be associated with the epithelial-to-mesenchymal transition and promote invasion and metastasis.

In lung adenocarcinomas, genes encoding the matrix metalloproteinases were upregulated in the *CXCR2/CXCR2* ligands cluster, as was the dual specificity phosphatase 4 (*DUSP4*) gene, which is known to be downregulated in *EGFR*-mutant NSCLC. Consistent with the association between poor differentiation and CXCR2 protein expression observed in the tissue microarray, another striking change was the downregulation of differentiation-associated genes, including thyroid transcription factor 1 (*NKX2-1*) (Supplementary Fig. 6A) and surfactant proteins B (*SFTPB*), C (*SFTPC*), and D (*SFTPD*), in the *CXCR2/*

CXCR2 ligands cluster. Interestingly, ribonucleotide reductase M2 (*RRM2*) was upregulated in the *CXCR2/CXCR2* ligands cluster, while folic acid receptor 1 (*FOLR1*) was downregulated. *RRM2* and *FOLR1* have been reported to modulate response to gemcitabine and pemetrexed, respectively, in NSCLC. Similar trends were observed in cell lines for *FOLR1* and *NKX2-1* downregulation (Supplementary Results and Supplementary Fig. 6B).

The most significant network associated with differential gene expression, with an absolute fold-change ≥0.5 between the *CXCR2/CXCR2* ligands cluster and the remaining samples, was related to *NFKB* in both the cell lines and lung adenocarcinoma (data not shown). Using as input the fold-change in gene expression between the *CXCR2/CXCR2* ligands cluster and the remaining lung adenocarcinomas, GSEA showed enrichment of genes associated with poor survival (Fig. 4C) (28). We also found enrichment in gene sets associated with poor differentiation and proliferation (data not shown), as well as MET transcriptionally coregulated genes (Fig. 4D). Using as input the fold-change in gene expression between the *CXCR2/CXCR2* ligands cluster and the remaining cell lines, GSEA showed a significant upregulation of gene sets related to the RAS pathway (Fig. 4E) and resistance to gefitinib (Fig. 4F), and enrichment of target genes of hsa-miR-let7, a known regulator of *KRAS* expression, and of genes associated with the epithelial-to-mesenchymal transition was observed (data not shown).

As an alternative approach to studying the effect of the *CXCR2/CXCR2* ligands axis, we summarized the effect of this axis by computing a principal components analysis (Supplementary Fig. 7A and 8A). The distribution of PC1 in cell lines was bimodal, a group of 12 cell lines having a high PC1 (≥1.5) and the remaining cell lines having a low PC1 (Supplementary Fig. 7B). Interestingly, cell line H1395, which has been reported to harbor an inactivating *CXCR2* G354W mutation, had a low PC1 (Supplementary Fig. 7B). Cell lines included in the *CXCR2/CXCR2* ligands cluster or with a high PC1 had low levels of *NKX2-1* gene expression, except HCC827 (Supplementary Fig. 7C).

In lung adenocarcinomas, a similar bimodal distribution of PC1 was observed (Supplementary Fig. 8A). Consistently with our immunohistochemical results, PC1 was statistically significantly higher in poorly differentiated adenocarcinomas than in moderately (P=0.0065) and well-differentiated tumors (P=0.0006) (Supplementary Fig. 8B), and higher in current smokers than in former (P=0.0010) and never smokers (P=0.0085) (Supplementary Fig. 8C). When PC1 was dichotomized based on the median, tumors with low PC1 were linked with longer OS (Fig. 3E); low PC1 was associated with HR of 0.6907 (95CI: 0.5302-0.9000, P-value=0.0061). After adjusting for patient age, sex, tumor stage, and institution, low PC1 remained associated with longer overall survival (HR of 0.6827; 95CI: 0.5046-0.8701, P=0.0031).

CXCL5 *is the main driver of the* CXCR2/CXCR2 ligands cluster in adenocarcinomas and is regulated through promoter methylation

CXCL5 was the gene most upregulated in the *CXCR2/CXCR2* ligands cluster in comparison to other samples across the whole genome, in both the cell lines and lung adenocarcinomas (Supplementary Results). *CXCL5* upregulation was associated with poor overall survival (Fig. 3F). Its distribution was bimodal in both cell lines and lung adenocarcinomas (Fig. 5A and B). This led us to hypothesize that promoter methylation might regulate its expression. *CXCL5* gene expression was inversely correlated with the average beta-value, which measures the degree of methylation of the promoter (Fig. 5C). Data generated in an independent study with publicly available raw data (32) confirmed high levels of expression of *CXCL5* in cell lines included in the *CXCR2/CXCR2* ligands axis, and low levels in other cell lines, including immortalized HBEC lines (Fig. 5D). Moreover, *CXCL5* expression was induced by decitabine in most of the cell lines with low *CXCL5*

expression that were shown to be methylated, as well as in HBEC cells. Expression of *CXCL1* (r = −0.46, *P*=0.0021), *CXCL2* (r = −0.49, *P*=0.0010), *CXCL3* (r = −0.32, *P*=0.0390), and *CXCL6* (r = −0.46, *P*=0.0022) genes was significantly inversely correlated with the average beta-value of their respective promoter, suggesting regulation through promoter methylation (Supplementary Fig. 9A-D). However, only *CXCL1* and *CXCL3* had patterns similar to *CXCL5* in terms of response to decitabine (Supplementary Fig. 10A-D).

Discussion

We demonstrate here that high level of cytoplasmic CXCR2 expression in tumor cells is associated with poor outcome, smoking, and poor tumor differentiation in patients with surgically resected stage I and II lung adenocarcinoma. Taking an alternative approach, we used publicly available gene expression profiles of a large set of NSCLC cell lines and lung adenocarcinomas to study the *CXCR2* axis. We identified a cluster of cell lines and lung adenocarcinomas we call the *CXCR2/CXCR2* ligands cluster, characterized by poor outcome, smoking, poor tumor differentiation, activation of *RAS* and MET pathways, epithelial-to-mesenchymal transition, and resistance to gefitinib. This cluster was driven mainly by CXCR2 ligand CXCL5, which was shown to be regulated through promoter methylation. We show that knocking down *CXCR2* in a cell line expressing high levels of *CXCR2* (344SQ) decreased its invasion potential *in vitro*, as well as tumor burden and metastatic potential *in vivo* in a novel orthotopic syngeneic lung adenocarcinoma metastasis model.

The role of CXCR2 in tumor cell proliferation has been reported in various tumor types: melanoma (20, 35), ovarian (36), prostate (37), and esophageal cancers (38). The promotion of cell proliferation by CXCR2 has been shown to involve an EGFR transactivation (17, 39) and increases in ERK1/2 (17, 38). Several studies have also reported that targeting CXCR2 inhibits tumor growth. Whether this effect is mediated mainly by inhibition of angiogenesis and/or by a direct effect on tumor cells remains unclear. Keane *et al.* studied the effect of CXCR2 using syngeneic murine Lewis lung cancer heterotopic and orthotopic tumor model systems in immunocompetent mice replete ($CXCR2^{+/+}$) or deficient in CXCR2 ($CXCR2^{-/-}$) (10). They reported a reduction in the tumor growth and metastatic potential of Lewis lung tumors in $CXCR2^{-/-}$ mice through a decrease of tumor angiogenesis. Using this model, the authors could appreciate the role of CXCR2 in host stromal cells.

To determine the direct effect of CXCR2 on the tumor deelopment, we used an orthotopic syngeneic lung cancer metastasis model using a highly metastatic cell line (344SQ) derived from $Kras^{LA1/+}p53^{R172H\Delta G/+}$ mice, which develop advanced ADC closely resemble the human disease (40). Knocking down *CXCR2* in shRNA stable clones created from 344SQ cell lines resulted in dramatic decreases of tumor burden, lymphatic and distant metastasis. This effect is unlikely to be related to a decrease in tumor angiogenesis, even though it has been reported that *CXCR2* knockdown in ovarian cancer cell lines injected subcutaneously can reduce tumor angiogenesis by suppressing TSP-1 and activating VEGF (36). We cannot completely exclude the possibility that *CXCR2* knockdown in the 344SQ cell line is associated with some degree of antiangiogenic effect.

We show in two large cohorts that both cytoplasmic CXCR2 (protein level) expression and the *CXCR2/CXCR2* ligands cluster (mRNA level) are associated with poor outcome. CXCR2 knockdown consistently decreased cell invasion *in vitro* as well as tumor burden and metastasis *in vivo*. Furthermore, a possible link between the CXCR2 pathway and the epithelial-to-mesenchymal transition has been suggested by others: Snail has been shown to promote CXCR2 ligand-dependent tumor progression in NSCLC (16, 41). Our GSEA analysis shows that the c-MET oncogenic pathway is enriched in the *CXCR2/CXCR2*

ligands cluster, consistent with our observation of downregulation of *SPINT1*, a potent inhibitor specific for HGF activator, and upregulation of *TGFB1* and *VIM* in the *CXCR2/CXCR2* ligands cluster (42).

These findings contrast with those of Ohri *et al.*, who studied the expression of CXCR2 in a small cohort of 20 NSCLC and reported its association with better outcome (43). This is in line with a report showing that depletion of CXCR2 delays both replicative senescence and impairs senescence response to oncogenic signals, suggesting that *CXCR2* acts as a tumor suppressor gene (21).

CXCR2 protein expression and the *CXCR2/CXCR2* ligands cluster were associated with poorly differentiated tumors. Interestingly, *NKX2-1* (*TTF-1*) was one of the genes most frequently downregulated in the cluster compared to other lung adenocarcinomas. NKX2-1 is a lineage-specific transcription factor. Its protein expression has been associated with a favorable prognosis. Approximately 30% of lung adenocarcinomas are negative for NKX2-1 (44). We envision that the absence of NKX2-1 protein expression might be a useful tool in identifying lung adenocarcinomas with activation of the *CXCR2* biological axis. This would have the advantage of simplicity, as NKX2-1 immunostaining is routine.

The *CXCR2/CXCR2* ligands cluster was driven mainly by *CXCL5*. The role of *CXCL5* in tumor progression is debated: it acts as a tumor suppressor in colon cancer (45), but has an oncogenic role in head and neck squamous cell carcinoma (46). A recent study reported methylation leading to silencing of *CXCL5* in over 75% of primary lung adenocarcinomas, but the authors did not report the effect of *CXCL5* expression on prognosis (47). We found a similar percentage (75-80%) of NSCLC cell lines and lung adenocarcinomas expressing low levels of *CXCL5* and show that this expression was regulated by promoter methylation. Based on the association of *CXCL5* with poor prognosis and its low expression in HBEC cell lines, we hypothesize that *CXCL5* might promote tumorigenesis in 20% of lung adenocarcinomas through CXCR2 autocrine and paracrine loop.

CXCR2 protein expression in NSCLC seems to be more associated KRAS mutation than EGFR mutation. In the DCC dataset, none of the lung adenocarcinomas included in the *CXCR2/CXCR2* ligands cluster had mutant *EGFR*. Cell lines included in this cluster were enriched in *KRAS* mutation,. Consistently, the *CXCR2/CXCR2* ligands cluster was enriched in gene sets related to the RAS pathway and resistance to gefitinib. The Let-7 family has been reported to regulate *KRAS* in lung cancer (48). Interestingly, genes downregulated by miR-let-7a-3 in the cell line A549, which harbors a *KRAS* mutation, were significantly enriched in the *CXCR2/CXCR2* ligands cluster *in vitro* (49). These observations, together with the dramatic effect of *CXCR2* knockdown in our orthotopic syngeneic lung adenocarcinoma metastasis model, which harbors a *KRAS* mutation, allow us to hypothesize that CXCR2 is an important target in *KRAS*-driven lung adenocarcinoma.

We previously showed that inflammatory cytokine IL-1β dramatically induced overexpression of several CXCR2 chemokine ligands (15). We also reported that alveolar epithelial cells transformed by oncogenic *KRAS* have high expression of CXCR2 ligands, which recruit inflammatory and endothelial cells and promote the progression of premalignant alveolar lesions to lung adenocarcinoma (8). CXCR2 is involved in the development of COPD, and CXCR2 inhibitors are currently being developed in this setting (7, 50). These observations suggest that CXCR2 inhibition might also be an interesting strategy for preventing lung cancer development in the high-risk smoking population by inhibiting early transformation of bronchial epithelial cells.

In conclusion, CXCR2 was shown to promote tumor cell invasion *in vitro* and tumor growth and metastasis in an orthotopic syngeneic lung adenocarcinoma metastasis model harboring

KRAS and *TP53* mutations. The *CXCR2* axis identifies a cluster of human NSCLC cell lines and lung adenocarcinomas, mostly driven by *CXCL5* and associated with poor prognosis, poor tumor differentiation, and smoking. *CXCL5* is shown to be regulated through promoter methylation. Together, these results suggest the *CXCR2-CXCL5* axis as a potential target in smoking-related lung adenocarcinomas.

Supplementary Material

Refer to Web version on PubMed Central for supplementary material.

Acknowledgments

Grant Support: National Cancer Institute grant R01-CA126801 (J.S.K.), Department of Defense VITAL grant W81XW-04-1-0142 (J.S.K., I.I.W., W.K.H.), Department of Defense IMPACT grant (J.S.K., I.I.W., W.K.H.), ASCO Conquer Cancer Foundation 2011 Young Investigator Award (E.M.), LUNG SPORE - P50 CA 70907 (J.M.K., I.I.W.), and NCI Cancer Center Support grant CA-16672 (The University of Texas MD Anderson Cancer Center) and CA-16359 (Yale Cancer Center).

References

1. Travis WD, Brambilla E, Noguchi M, Nicholson AG, Geisinger KR, Yatabe Y, et al. International association for the study of lung cancer/american thoracic society/european respiratory society international multidisciplinary classification of lung adenocarcinoma. J Thorac Oncol. 2011; 6:244–85. [PubMed: 21252716]
2. Pao W, Girard N. New driver mutations in non-small-cell lung cancer. Lancet Oncol. 2011; 12:175–80. [PubMed: 21277552]
3. Suda K, Tomizawa K, Yatabe Y, Mitsudomi T. Lung cancers unrelated to smoking: characterized by single oncogene addiction? Int J Clin Oncol. 2011; 16:294–305. [PubMed: 21655907]
4. Paik PK, Arcila ME, Fara M, Sima CS, Miller VA, Kris MG, et al. Clinical characteristics of patients with lung adenocarcinomas harboring BRAF mutations. J Clin Oncol. 2011; 29:2046–51. [PubMed: 21483012]
5. Balkwill F. Cancer and the chemokine network. Nat Rev Cancer. 2004; 4:540–50. [PubMed: 15229479]
6. Chapman RW, Phillips JE, Hipkin RW, Curran AK, Lundell D, Fine JS. CXCR2 antagonists for the treatment of pulmonary disease. Pharmacol Ther. 2009; 121:55–68. [PubMed: 19026683]
7. Johnson Z, Power CA, Weiss C, Rintelen F, Ji H, Ruckle T, et al. Chemokine inhibition--why, when, where, which and how? Biochem Soc Trans. 2004; 32:366–77. [PubMed: 15046611]
8. Wislez M, Fujimoto N, Izzo JG, Hanna AE, Cody DD, Langley RR, et al. High expression of ligands for chemokine receptor CXCR2 in alveolar epithelial neoplasia induced by oncogenic kras. Cancer Res. 2006; 66:4198–207. [PubMed: 16618742]
9. Strieter RM, Burdick MD, Gomperts BN, Belperio JA, Keane MP. CXC chemokines in angiogenesis. Cytokine Growth Factor Rev. 2005; 16:593–609. [PubMed: 16046180]
10. Keane MP, Belperio JA, Xue YY, Burdick MD, Strieter RM. Depletion of CXCR2 inhibits tumor growth and angiogenesis in a murine model of lung cancer. J Immunol. 2004; 172:2853–60. [PubMed: 14978086]
11. Raghuwanshi SK, Nasser MW, Chen X, Strieter RM, Richardson RM. Depletion of beta-arrestin-2 promotes tumor growth and angiogenesis in a murine model of lung cancer. J Immunol. 2008; 180:5699–706. [PubMed: 18390755]
12. Burger M, Burger JA, Hoch RC, Oades Z, Takamori H, Schraufstatter IU. Point mutation causing constitutive signaling of CXCR2 leads to transforming activity similar to Kaposi's sarcoma herpesvirus-G protein-coupled receptor. J Immunol. 1999; 163:2017–22. [PubMed: 10438939]
13. Vandercappellen J, Van Damme J, Struyf S. The role of CXC chemokines and their receptors in cancer. Cancer Lett. 2008; 267:226–44. [PubMed: 18579287]
14. Zhu YM, Webster SJ, Flower D, Woll PJ. Interleukin-8/CXCL8 is a growth factor for human lung cancer cells. Br J Cancer. 2004; 91:1970–6. [PubMed: 15545974]

15. Sun H, Chung WC, Ryu SH, Ju Z, Tran HT, Kim E, et al. Cyclic AMP-responsive element binding protein- and nuclear factor-kappaB-regulated CXC chemokine gene expression in lung carcinogenesis. Cancer Prev Res (Phila). 2008; 1:316–28. [PubMed: 19138976]
16. Yanagawa J, Walser TC, Zhu LX, Hong L, Fishbein MC, Mah V, et al. Snail promotes CXCR2 ligand-dependent tumor progression in non-small cell lung carcinoma. Clin Cancer Res. 2009; 15:6820–9. [PubMed: 19887480]
17. Luppi F, Longo AM, de Boer WI, Rabe KF, Hiemstra PS. Interleukin-8 stimulates cell proliferation in non-small cell lung cancer through epidermal growth factor receptor transactivation. Lung Cancer. 2007; 56:25–33. [PubMed: 17175059]
18. Maxwell PJ, Gallagher R, Seaton A, Wilson C, Scullin P, Pettigrew J, et al. HIF-1 and NF-kappaB-mediated upregulation of CXCR1 and CXCR2 expression promotes cell survival in hypoxic prostate cancer cells. Oncogene. 2007; 26:7333–45. [PubMed: 17533374]
19. Varney ML, Singh S, Li A, Mayer-Ezell R, Bond R, Singh RK. Small molecule antagonists for CXCR2 and CXCR1 inhibit human colon cancer liver metastases. Cancer Lett. 2010; 300:180–8. [PubMed: 21035946]
20. Singh S, Sadanandam A, Nannuru KC, Varney ML, Mayer-Ezell R, Bond R, et al. Small-molecule antagonists for CXCR2 and CXCR1 inhibit human melanoma growth by decreasing tumor cell proliferation, survival, and angiogenesis. Clin Cancer Res. 2009; 15:2380–6. [PubMed: 19293256]
21. Acosta JC, O'Loghlen A, Banito A, Guijarro MV, Augert A, Raguz S, et al. Chemokine signaling via the CXCR2 receptor reinforces senescence. Cell. 2008; 133:1006–18. [PubMed: 18555777]
22. Gibbons DL, Lin W, Creighton CJ, Rizvi ZH, Gregory PA, Goodall GJ, et al. Contextual extracellular cues promote tumor cell EMT and metastasis by regulating miR-200 family expression. Genes Dev. 2009; 23:2140–51. [PubMed: 19759262]
23. Yang Y, Ahn YH, Gibbons DL, Zang Y, Lin W, Thilaganathan N, et al. The Notch ligand Jagged2 promotes lung adenocarcinoma metastasis through a miR-200-dependent pathway in mice. J Clin Invest. 2011; 121:1373–85. [PubMed: 21403400]
24. Zheng S, El-Naggar AK, Kim ES, Kurie JM, Lozano G. A genetic mouse model for metastatic lung cancer with gender differences in survival. Oncogene. 2007; 26:6896–904. [PubMed: 17486075]
25. Yuan P, Kadara H, Behrens C, Tang X, Woods D, Solis LM, et al. Sex determining region Y-Box 2 (SOX2) is a potential cell-lineage gene highly expressed in the pathogenesis of squamous cell carcinomas of the lung. PLoS One. 2010; 5:e9112. [PubMed: 20161759]
26. Ijichi H, Chytil A, Gorska AE, Aakre ME, Bierie B, Tada M, et al. Inhibiting Cxcr2 disrupts tumor-stromal interactions and improves survival in a mouse model of pancreatic ductal adenocarcinoma. J Clin Invest. 2011; 121:4106–17. [PubMed: 21926469]
27. White JR, Lee JM, Young PR, Hertzberg RP, Jurewicz AJ, Chaikin MA, et al. Identification of a potent, selective non-peptide CXCR2 antagonist that inhibits interleukin-8-induced neutrophil migration. J Biol Chem. 1998; 273:10095–8. [PubMed: 9553055]
28. Shedden K, Taylor JM, Enkemann SA, Tsao MS, Yeatman TJ, Gerald WL, et al. Gene expression-based survival prediction in lung adenocarcinoma: a multi-site, blinded validation study. Nat Med. 2008; 14:822–7. [PubMed: 18641660]
29. Lockwood WW, Chari R, Coe BP, Girard L, Macaulay C, Lam S, et al. DNA amplification is a ubiquitous mechanism of oncogene activation in lung and other cancers. Oncogene. 2008; 27:4615–24. [PubMed: 18391978]
30. Zhou BB, Peyton M, He B, Liu C, Girard L, Caudler E, et al. Targeting ADAM-mediated ligand cleavage to inhibit HER3 and EGFR pathways in non-small cell lung cancer. Cancer Cell. 2006; 10:39–50. [PubMed: 16843264]
31. Raponi M, Zhang Y, Yu J, Chen G, Lee G, Taylor JM, et al. Gene expression signatures for predicting prognosis of squamous cell and adenocarcinomas of the lung. Cancer Res. 2006; 66:7466–72. [PubMed: 16885343]
32. Shames DS, Girard L, Gao B, Sato M, Lewis CM, Shivapurkar N, et al. A genome-wide screen for promoter methylation in lung cancer identifies novel methylation markers for multiple malignancies. PLoS Med. 2006; 3:e486. [PubMed: 17194187]

33. Onn A, Isobe T, Itasaka S, Wu W, O'Reilly MS, Ki Hong W, et al. Development of an orthotopic model to study the biology and therapy of primary human lung cancer in nude mice. Clin Cancer Res. 2003; 9:5532–9. [PubMed: 14654533]
34. Roybal JD, Zang Y, Ahn YH, Yang Y, Gibbons DL, Baird BN, et al. miR-200 Inhibits lung adenocarcinoma cell invasion and metastasis by targeting Flt1/VEGFR1. Mol Cancer Res. 2011; 9:25–35. [PubMed: 21115742]
35. Singh S, Varney M, Singh RK. Host CXCR2-dependent regulation of melanoma growth, angiogenesis, and experimental lung metastasis. Cancer Res. 2009; 69:411–5. [PubMed: 19147552]
36. Yang G, Rosen DG, Liu G, Yang F, Guo X, Xiao X, et al. CXCR2 promotes ovarian cancer growth through dysregulated cell cycle, diminished apoptosis, and enhanced angiogenesis. Clin Cancer Res. 2010; 16:3875–86. [PubMed: 20505188]
37. Murphy C, McGurk M, Pettigrew J, Santinelli A, Mazzucchelli R, Johnston PG, et al. Nonapical and cytoplasmic expression of interleukin-8, CXCR1, and CXCR2 correlates with cell proliferation and microvessel density in prostate cancer. Clin Cancer Res. 2005; 11:4117–27. [PubMed: 15930347]
38. Wang B, Hendricks DT, Wamunyokoli F, Parker MI. A growth-related oncogene/CXC chemokine receptor 2 autocrine loop contributes to cellular proliferation in esophageal cancer. Cancer Res. 2006; 66:3071–7. [PubMed: 16540656]
39. Bolitho C, Hahn MA, Baxter RC, Marsh DJ. The chemokine CXCL1 induces proliferation in epithelial ovarian cancer cells by transactivation of the epidermal growth factor receptor. Endocr Relat Cancer. 2010; 17:929–40. [PubMed: 20702723]
40. Jackson EL, Olive KP, Tuveson DA, Bronson R, Crowley D, Brown M, et al. The differential effects of mutant p53 alleles on advanced murine lung cancer. Cancer Res. 2005; 65:10280–8. [PubMed: 16288016]
41. Kuo PL, Chen YH, Chen TC, Shen KH, Hsu YL. CXCL5/ENA78 increased cell migration and epithelial-to-mesenchymal transition of hormone-independent prostate cancer by early growth response-1 /Snail signaling pathway. J Cell Physiol. 2010
42. Roussos ET, Keckesova Z, Haley JD, Epstein DM, Weinberg RA, Condeelis JS. AACR special conference on epithelial-mesenchymal transition and cancer progression and treatment. Cancer Res. 2010; 70:7360–4. [PubMed: 20823151]
43. Ohri CM, Shikotra A, Green RH, Waller DA, Bradding P. Chemokine receptor expression in tumour islets and stroma in non-small cell lung cancer. BMC Cancer. 2010; 10:172. [PubMed: 20429924]
44. Tang X, Kadara H, Behrens C, Liu DD, Xiao Y, Rice D, et al. Abnormalities of the TITF-1 lineage-specific oncogene in NSCLC: implications in lung cancer pathogenesis and prognosis. Clin Cancer Res. 2011; 17:2434–43. [PubMed: 21257719]
45. Speetjens FM, Kuppen PJ, Sandel MH, Menon AG, Burg D, van de Velde CJ, et al. Disrupted expression of CXCL5 in colorectal cancer is associated with rapid tumor formation in rats and poor prognosis in patients. Clin Cancer Res. 2008; 14:2276–84. [PubMed: 18413816]
46. Miyazaki H, Patel V, Wang H, Edmunds RK, Gutkind JS, Yeudall WA. Down-regulation of CXCL5 inhibits squamous carcinogenesis. Cancer Res. 2006; 66:4279–84. [PubMed: 16618752]
47. Tessema M, Klinge DM, Yingling CM, Do K, Van Neste L, Belinsky SA. Re-expression of CXCL14, a common target for epigenetic silencing in lung cancer, induces tumor necrosis. Oncogene. 2010; 29:5159–70. [PubMed: 20562917]
48. Johnson SM, Grosshans H, Shingara J, Byrom M, Jarvis R, Cheng A, et al. RAS is regulated by the let-7 microRNA family. Cell. 2005; 120:635–47. [PubMed: 15766527]
49. Brueckner B, Stresemann C, Kuner R, Mund C, Musch T, Meister M, et al. The human let-7a-3 locus contains an epigenetically regulated microRNA gene with oncogenic function. Cancer Res. 2007; 67:1419–23. [PubMed: 17308078]
50. Holz O, Khalilieh S, Ludwig-Sengpiel A, Watz H, Stryszak P, Soni P, et al. SCH527123, a novel CXCR2 antagonist, inhibits ozone-induced neutrophilia in healthy subjects. Eur Respir J. 2009; 35:564–70. [PubMed: 19643947]

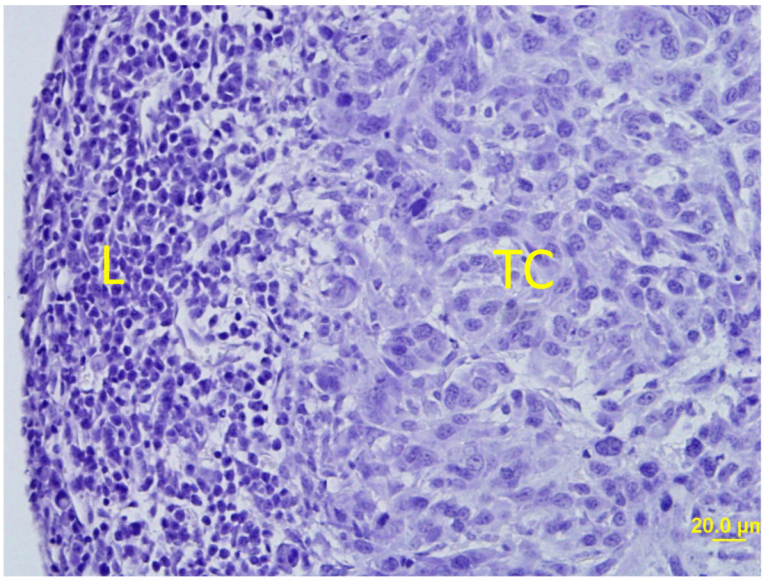

Figure 1. Mediastinal lymph node metastasis from an orthotopic lung tumor

Hematoxylin and eosin-stained tissue section of a mediastinal lymph node from a mouse injected intra-thoracically (left lung) with 344SQ cells (2×10^4), killed after 21 days, and subjected to necropsy (L: lymphocytes; TC: tumor cells).

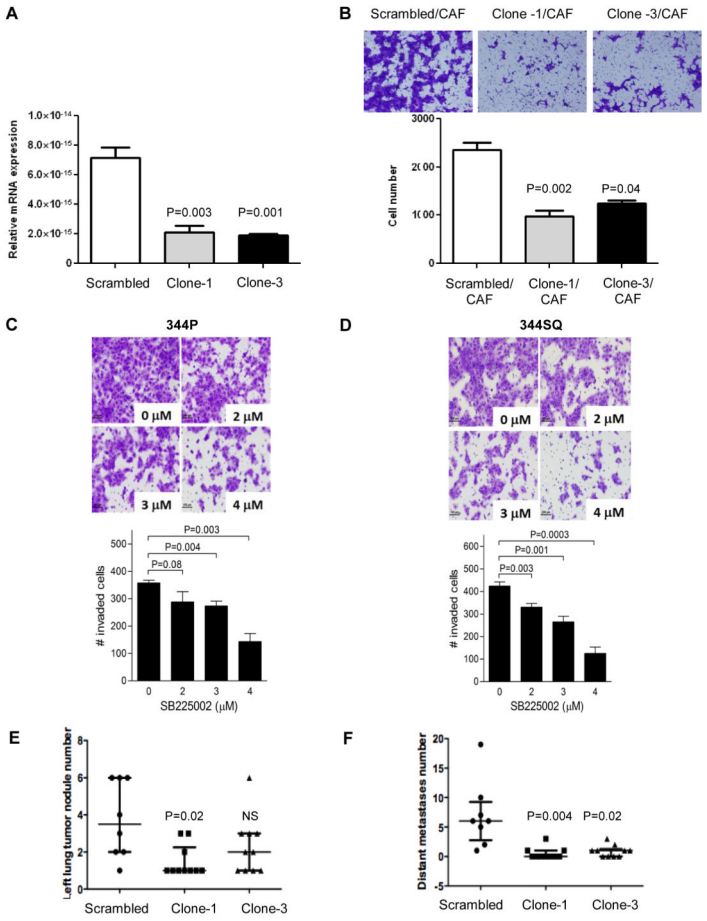

Figure 2. Effect of CXCR2 downregulation and inhibition

In vitro (A-B) properties of shRNA clones (clone-1 and -3) compared to scrambled control: (A) mRNA expression by reverse-transcription PCR relative to standard, (B) invasion assay using co-cultures with cancer-associated fibroblasts (CAF) and mitomycin C to block tumor cell proliferation. *In vitro* CXCR2 inhibition with CXCR2-antagonist (C, D): invasion assay using co-cultures of 344P (C) and 344SQ (D) cell lines treated with increasing concentrations of SB225002.*In vivo* properties of shRNA clones (clone-1 and -3) compared to scrambled control (E, F): number of left lung tumor nodules, (E) number of distant metastases (F). Median and inter-quartile range are shown in the dot plots (E, F). Wilcoxon rank sum test (A, B, E, and F) between scrambled control and shRNA single clones (clone-1 and clone-3) or between different concentrations of SB225002and the control (C, D).

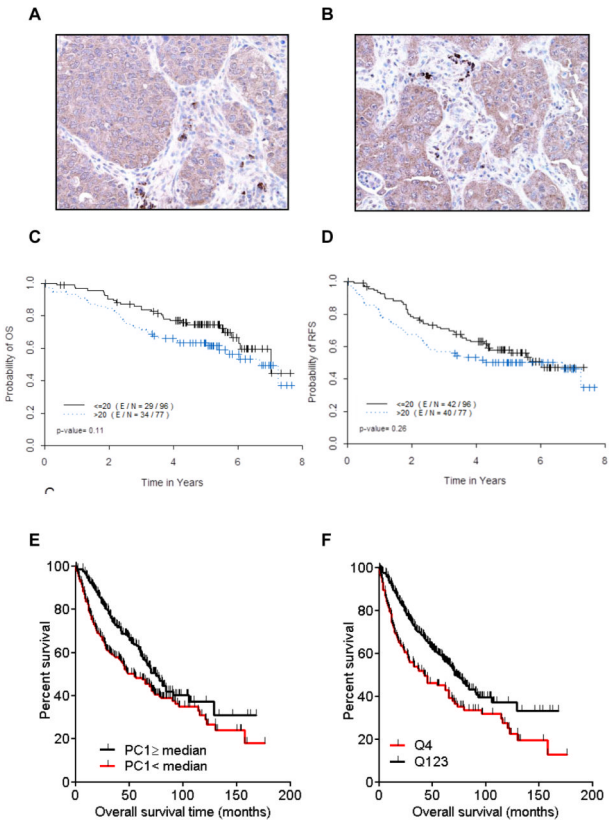

Figure 3. Expression of CXCR2 and its ligands in tumor cells and tissues

CXCR2 axis and *CXCL5* expression are associated with poor outcome. Immunohistochemical expression of CXCR2 in two NSCLC tissue specimens, (A) squamous cell carcinoma and (B) adenocarcinoma. Kaplan-Meier curves for (C) overall survival and (D) recurrence-free survival as a function of cytoplasmic CXCR2 expression in 173 patients who underwent resection for lung adenocarcinoma. (E) First principal component (PC1) was computed with expression of the *CXCR2* genes and its ligand genes (*CXCL6, IL8, CXCL2, CXCL1, CXCL3, CXCL7*, and *CXCL5*); Kaplan-Meier curves for overall survival among patients with high versus low PC1 based on the median. (F) Kaplan-Meier curves for overall survival for patients with high (highest quartile) versus low (lowest quartile) *CXCL5* gene expression.

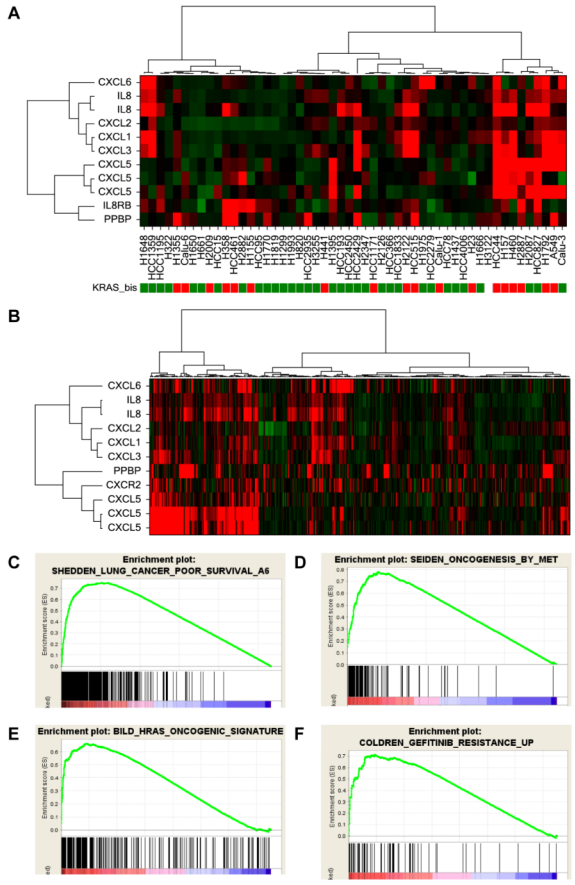

Figure 4. Identification of a *CXCR2/CXCR2* ligands cluster

Unsupervised clustering using gene expression of *CXCR2* and its ligands (*CXCL6, IL8, CXCL2, CXCL1, CXCL3, PPBP [CXCL7]*, and *CXCL5*) in (A) 52 NSCLC cell lines and (B) 442 lung adenocarcinomas. For Gene Set Enrichment Analysis, genes were preranked according to the fold-change observed between samples with the *CXCR2/CXCR2* ligands cluster and the remaining samples in both lung adenocarcinomas (C, D) and cell lines (E, F); representative gene sets enriched with a *P*-value and a false discovery rate <0.0001 are shown for lung adenocarcinomas (C, D) and NSCLC cell lines (E, F).

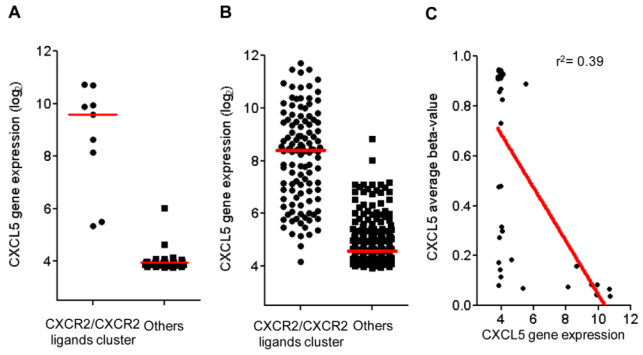

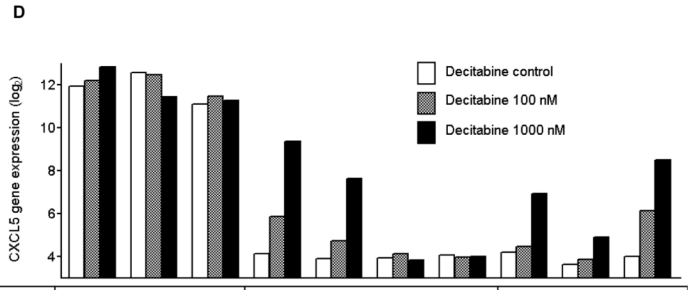

Cell line	A549	H157	H460	H1299	H2347	H1819	H1993	HBEC2	HBEC3	HBEC4
% methyl.	8%	16%	8%	87%	94%	94%	94%	NA	NA	NA
	CXCR2/CXCR2 ligands cluster			Other cell lines				Immortalized bronchial epithelial cell lines		

Figure 5. *CXCL5* drives the *CXCR2/CXCR2* ligands cluster and is regulated through promoter methylation

CXCL5 is the gene most frequently upregulated across the whole genome in samples with the *CXCR2/CXCR2* ligands cluster compared to other samples, both *in vitro* (A) and *in vivo* (B). (C) *CXCL5* gene expression was inversely correlated with the average beta-value, and (D) was increased after treatment with decitabine in most of the cell lines with low baseline *CXCL5* expression.

Table 1

Clinical and pathological characteristics of patients included in the tissue microarrj (N=262)

Covariate	N (%)
Sex	
F	134(51.1%)
M	128(48.9%)
Race	
Other	22(8.4%)
White	240(91.6%)
Smoking status	
Current	105(40.1%)
Former	127(48.5%)
Never	30(11.5%)
Pathological stage	
I	201(76.7%)
II	61(23.3%)
Histology	
Adenocarcinoma	173(66%)
Squamous cell carcinoma	89(34%)
Degree of differentiation	
Poor	74(28.2%)
Moderate	155(59.2%)
Well	33(12.6%)
Degree of inflammation	
Mild	106(41.1%)
Moderate	106(41.1%)
Severe	46(17.8%)
Unknown	4
Adjuvant therapy	
No	180(71.4%)
Yes	72(28.6%)
Unknown	10

Cancer Res. Author manuscript; available in PMC 2014 January 15.

Table 2

Final multicovariate Cox models assessing the effect of covariates on overall survival in the whole population (N=262) (A), in patients with lung adenocarcinoma (N=173) (B), and in patients with lung squamous cell carcinoma (N=89) (C) (M: male; F: female; HR: hazard ratio; CI: confidence interval)

A

	Analysis of Maximum Likelihood Estimates					
Parameter	***Parameter Estimate***	***Standard Error***	***P-value***	***HR***	***95% HR CI***	
age	0.02214	0.01048	0.0346	1.022	1.002	1.044
Gender (M vs. F)	0.38869	0.20544	0.0585	1.475	0.986	2.206
Stage (II vs. I)	0.49491	0.22793	0.0299	1.640	1.049	2.564
CXCR2 (>20 vs.<=20)	0.44397	0.20116	0.0273	1.559	1.051	2.312

B

	Analysis of Maximum Likelihood Estimates					
Parameter	*Parameter Estimate*	*Standard Error*	*P-value*	*HR*	*95% HR CI*	
age	0.02064	0.01273	0.1049	1.021	0.996	1.047
Gender (M vs. F)	0.62208	0.25904	0.0163	1.863	1.121	3.095
Stage (II vs. I)	0.72598	0.28779	0.0116	2.067	1.176	3.633
CXCR2 (>20 vs. <=20)	0.34171	0.25741	0.1843	1.407	0.850	2.331

C

	Analysis of Maximum Likelihood Estimates					
Parameter	*Parameter Estimate*	*Standard Error*	*P-value*	*HR*	*95% HR CI*	
age	0.02065	0.01939	0.2869	1.021	0.983	1.060

A

Analysis of Maximum Likelihood Estimates						
Parameter	***Parameter Estimate***	***Standard Error***	***P-value***	***HR***	***95% HR CI***	
Gender (M vs. F)	0.05144	0.35478	0.8847	1.053	0.525	2.110
Stage (II vs. I)	0.20288	0.39319	0.6059	1.225	0.567	2.647
CXCR2 (>20 vs. <=20)	0.46527	0.33894	0.1698	1.592	0.820	3.094